International Journal of Smart Grid and Clean Energy

Co-ordinated frequency droop-based power sharing strategy of resilient microgrids through DC grid

Mir Nahidul Ambia[a], Ke Meng[b], Weidong Xiao[a] , Zhao Yang Dong[b]

[a] *The University of Sydney, Sydney,2006, NSW, Australia*
[b] *The University of New South Wales, Sydney, 2052, NSW, Australia*

Abstract

The paper presents a networked microgrid system, where droop-based frequency regulation has been implemented on *PQ* control of inverters. During transition from grid mode to islanding mode, the networked microgrid faces extreme disturbances, which requires proper sharing within the network. In this paper, a networked microgrid topology is analysed, where power sharing occurs through the dc network. Moreover, proposed controller activates a droop sharing strategy, which identifies required active power for frequency regulation before entering to islanding stages. However, during power sharing case, microgrid capable of extracting additional power uses the droop control, while other network inverter utilizes dc link voltage, resulting calculation of overall reference inverter current for proper sharing. Furthermore, the controller co-ordinates between different microgrids based on the reference current to enhance the resilience of the network. The effectiveness of the illustrated control is unique, as the power sharing occurs via dc grid, thus, it has been tested on PSCAD with test cases.

Keywords: Droop control, microgrids, power sharing, resilience.

1. Introduction

High rate of renewable energy integration into the modern power system is instrumental indeed. Though it has got numerous benefits in terms of grid resilience, the power system is still looking for convenient solutions. Loss of generation, natural disasters have shown that a feasible solution is yet to be achieved. Modern power system has stepped into modern microgrid, which is aimed to depend on renewable energy resources. Modern microgrid, which runs on grid and islanded modes, requires smooth transition in case of power grid failure [1-4].

Though the dependency on power grid is salient, its downside cannot be ignored; nevertheless, the contradiction is rooted in the fact that due to loss of power grid, microgrid still needs to enhance its resilience. Studies have shown numerous solutions on power grid resilience. A hierarchical control of droop for hybrid microgrids have been proposed in [5]. A power management strategy is proposed in [6], which aims to balance in the network system. Moreover, [7] illustrates self-healing resilient distribution systems based on sectionalisation into microgrids. Harmony search algorithm-based controllers are applied in microgrid system in [8]. Dynamic multicriteria decision making is implemented for coupling neighbouring microgrids in [9]. Centralized and decentralized methods are presented as feasible solution for DC and hybrid microgrids in [10-11]. Frequency control in islanded microgrids through voltage regulation is proposed in [12], while self-healing control is depicted in [13].

The above presented research papers identify a feasible solution, however networked microgrids consist of more than one microgrid, require further analysis with inverters. Moreover, the networked microgrids allow power transfer through ac and dc grid. In this paper, the networked microgrid topology uses ac microgrids, however they are connected on the common dc terminal. Thus, power transfer is

* Manuscript received May, 6, 2019; revised February 7, 2020.
doi: 10.12720/sgce.9.2.247-254

analyzed through DC grid only, which provides opportunity for a feasible solution. Furthermore, co-ordination between inverters require certain control strategy to uplift the resilience of power system. Hence, this paper presents a novel droop control, which maintains frequency regulation along with additional power adjustment to balance the network. It also provides a solution between two inverters set, where one set aims for additional power to the load, while other one follows dc-link voltage control. The system network is shown in section 2. The modelling of inverters is shown in section 3, while control strategy is further explained in section 4. Section 5 shows the simulation results with test cases on PSCAD platform.

2. System Network

A typical networked microgrid system has been shown in Fig. 1, which consists several microgrid setup, each containing renewable energy resources and ac loads. The whole network is connected to a power grid. Microgrid 1 and 3 extracts power through the wind farm, while other networks generate power through the slack bus. Four inverters are connected in parallel, which mounts on the common point of dc grid. Once main power grid is islanded, the networked microgrid depends on its local individual power sources, however, due to absence of power grid, networked microgrid is supposed to share active power through the DC grid.

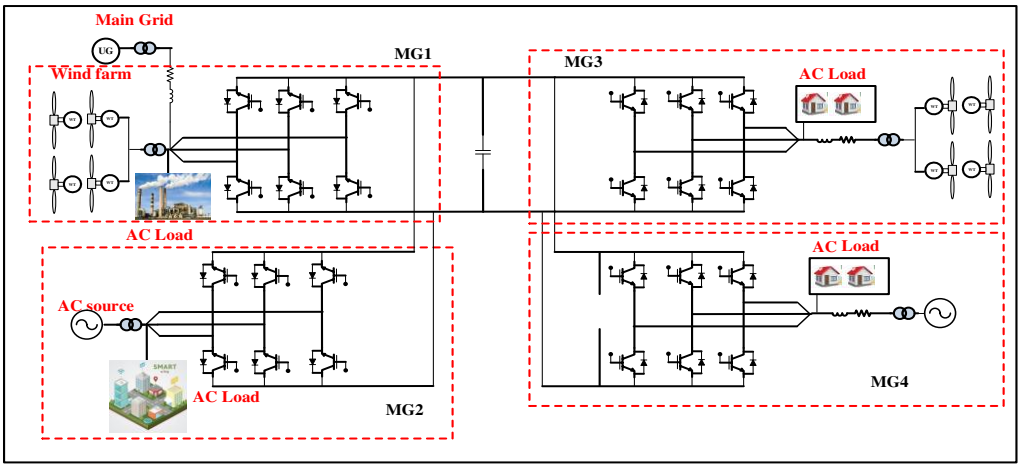

Fig. 1. Networked microgrid system connected on parallel inverters through common dc grid

3. Network Microgrids Converter Modelling

A voltage source converter referred as interlinking converter (IC) has been modelled in the networked microgrid system which is applied in each level microgrid operating by pulse width modulation pulses from the proposed controller as per Fig. 1. The converter provides active and reactive power support to stabilize the networked microgrid system. The converter side voltages are V_a, V_b, V_c. The converter is connected at the point of utility grid and wind farm set (E_{ag}, E_{bg}, E_{cg} for grid side voltage and E_{aMg}, E_{bMg}, E_{cMg} for microgrid side voltage). From the circuit diagram and by applying Kirchhoff's voltage law, following equation can be formulated, where resistance R and inductor L is connected between converter and microgrid.

$$E_{ag} + E_{aMg} = L_a \frac{dI_a}{dt} + R_a I_a + V_a \tag{1}$$

$$E_{bg} + E_{bMg} = L_b \frac{dI_b}{dt} + R_b I_b + V_b \tag{2}$$

$$E_{cg} + E_{cMg} = L_c \frac{dI_c}{dt} + R_c I_c + V_c \tag{3}$$

Using Park's transformation, *abc* frame can be converted to *d-q* axis voltage, which provides below equations.

$$E_{dg} + E_{dMg} = L\frac{dI_d}{dt} + RI_d + V_d - 2\pi fLI_q \tag{4}$$

$$E_{qg} + E_{qMg} = L\frac{dI_q}{dt} + RI_q + V_q - 2\pi fLI_d \tag{5}$$

where, E_{dg} & E_{qg} are d-q axis voltages for grid side. E_{dMg} & E_{qMg} are d-q axis voltages for networked microgrids. In *abc* to *dq0* transformation, the transformed *d-q* voltage is controlled such a way that it synchronizes with main voltage. However, the angle of main voltage is in same phase with d-axis voltage, which makes the q component of grid & microgrid voltage zero. Assuming, E_{qg}+E_{qMg}=0, the derivatives of I_d and I_q can be found.

$$\frac{dI_d}{dt} = \frac{E_{dg} + E_{dMg}}{L} - \frac{R}{L}I_d - \frac{V_d}{L} + 2\pi fI_q \tag{6}$$

$$\frac{dI_q}{dt} = -\frac{R}{L}I_d - \frac{V_d}{L} + 2\pi fI_d \tag{7}$$

4. Proposed Control

The proposed control is implemented on the classical PQ controller, where active and reactive power is controlled on d-axis and q-axis respectively. However, the contradiction is rooted in the fact that classical control is unable to provide additional active power during islanding stage. Moreover, the power sharing through dc network requires certain amount of co-ordination to balance the overall active power in the network.

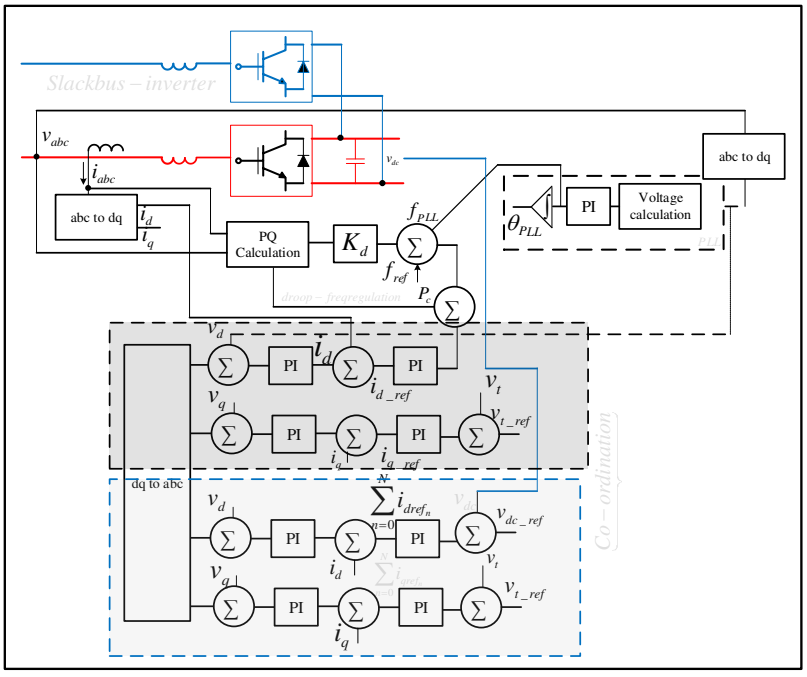

Fig. 2. Proposed co-ordinated droop-based frequency regulation system.

4.1. Frequency droop regulation

As mentioned before, the proposed control is a modification of classical PQ control. That being said, a droop co-efficient is used in the converter, which aims to extract additional power during power shortage though the respective power source. Fig. 2 reflects the proposed control, where two inverters from separate microgrids are indicated in single line diagram. The red coloured inverter is the one that aims to provide additional power. Thus, it measures voltage and current signal to calculate necessary active and reactive power. Through the droop equation as indicated in Eqn. (8), it takes frequency input either through the PLL or through the speed measurement of respective generators. The aim is to control the frequency and generate certain reference inverter current to enhance the resilience.

$$i_{d1\_ref} = k_{p_1}\left[\left(p_{c1}^{*} - p_{c1}\right) + \left(k_{p_5}\left\{f_1^{ref} - p_{c1}k_{d1} - f_1(t)\right\} + k_{i_5}\int_0^t \left\{f_1^{ref} - p_{c1}k_{d1} - f_1(t)\right\}.d\tau\right)\right] + k_{i_1}\int_0^t\left[\left(p_{c1}^{*} - p_{c1}\right) + \left(k_{p_5}\left\{f_1^{ref} - p_{c1}k_{d1} - f_1(t)\right\} + k_{i_5}\int_0^t \left\{f_1^{ref} - p_{c1}k_{d1} - f_1(t)\right\}.d\tau\right)\right].d\tau \tag{8}$$

The regulation through the PI controller takes inverter power as a reference to generate the i_{dref} current. The reference is compared with measured i_d current to minimize the error.

Furthermore, for inverters with slack bus are designed to control the dc link voltage as it does not require to control the frequency. Based on the similar principle explained above the reference current for the inverters on d-axis are mathematically formulated below.

$$i_{dref} = k_{p_1}\left[\left(V_{dc}^{*} - V_{dc}\right)\right] + k_{i_1}\int_0^t\left[\left(V_{dc}^{*} - V_{dc}\right)\right].d\tau \tag{9}$$

4.2. Outer-loop control

In the outer-loop control, the output of inner loop is sent though a PI controller and added with v_d, which is d-axis voltage of line voltage. It is added to track with system voltage. The output of PI controller generates the reference voltage v_{dref} as indicated in Eqns (10-11).

$$v_d = 2/3\left[v_a\cos(\omega t) + v_b\cos(\omega t - \theta) + v_c\cos(\omega t + \theta)\right] \tag{10}$$

$$v_{dref} = k_{p_3}\left[i_{dref} - i_d\right] + k_{i_3}\int_0^t\left[i_{dref}(t) - i_d(t)\right].d\tau + v_d \tag{11}$$

Eqn. (8) can be further replaced with Eqn. (10, 11), which results in Eqn. (12).

$$v_{dref} = k_{p_3}\left[\left[\begin{array}{l} k_{p_1}\left[\left(p_c^{*} - p_c\right) + \left(k_{p_5}\left\{f^{ref} - p_c k_d - f(t)\right\} + k_{i_5}\int_0^t\left\{f^{ref} - p_c k_d - f(t)\right\}.d\tau\right)\right] + \\ k_{i_1}\int_0^t\left[\left(p_c^{*} - p_c\right) + \left(k_{p_5}\left\{f^{ref} - p_c k_d - f(t)\right\} + k_{i_5}\int_0^t\left\{f^{ref} - p_c k_d - f(t)\right\}.d\tau\right)\right].d\tau \end{array}\right] - i_d\right] + k_{i_3}\int_0^t\left[\left[\begin{array}{l} k_{p_1}\left[\left(p_c^{*} - p_c\right) + \left(k_{p_5}\left\{f^{ref} - p_c k_d - f(t)\right\} + k_{i_5}\int_0^t\left\{f^{ref} - p_c k_d - f(t)\right\}.d\tau\right)\right] + \\ k_{i_1}\int_0^t\left[\left(p_c^{*} - p_c\right) + \left(k_{p_5}\left\{f^{ref} - p_c k_d - f(t)\right\} + k_{i_5}\int_0^t\left\{f^{ref} - p_c k_d - f(t)\right\}.d\tau\right)\right].d\tau \end{array}\right] - i_d(t)\right].d\tau + \left[2/3\left[v_a\cos(\omega t) + v_b\cos(\omega t - \theta) + v_c\cos(\omega t + \theta)\right]\right] \tag{12}$$

4.3. Co-ordinated power sharing

The co-ordinated power sharing is activated by injection of all d-axis reference currents to adjust the

frequency along with active power and dc link voltage. Furthermore, the reactive power compensation is achieved by q-axis current injection by the inverters. However, to control the active power in this system can be achieved by co-ordination between all inverters through proper d-axis current injection. As indicated earlier, Eqns. (8) and (9) contribute both into the system to keep the system stable. The reference current of certain inverter illustrated as Eqn. (9) is modified into Eqn. (13) for a larger network.

$$\sum_{n=0}^{N} i_{dref_n} = k_{p_1}\left[\sum_{n=0}^{N}\left(V_{dc_n}^{*} - V_{dc_n}\right)\right] + k_{i_1}\int_0^t\left[\sum_{n=0}^{N}\left(V_{dc_n}^{*} - V_{dc_n}\right)\right]d\tau \tag{13}$$

To build a relation between two separate reference current injection, Eqn. (14) is shown, which provides a relation between two different system dynamics. It can be understood that the co-ordination takes place once certain variables individually satisfy the requirement. In addition, it provides total injection intro the network, which aims for frequency regulation and dc-link voltage control. In contrast, the injection participates actively in the control of active in the network to meet the load demand in the networked microgrid system. The references are adjusted accordingly in the system for enhanced resiliency of the networked microgrid system.

$$i_{d1\_ref} + \sum_{n=0}^{N} i_{dref_n} = \left[\underbrace{\begin{array}{l} k_{p_1}\left[\left(p_{c1}^{*} - p_{c1}\right) + \left(k_{p_5}\left\{f_1^{ref} - p_{c1}k_{d1} - f_1(t)\right\} + k_{i_5}\int_0^t\left\{f_1^{ref} - p_{c1}k_{d1} - f_1(t)\right\}.d\tau\right)\right] + \\ k_{i_1}\int_0^t\left[\left(p_{c1}^{*} - p_{c1}\right) + \left(k_{p_5}\left\{f_1^{ref} - p_{c1}k_{d1} - f_1(t)\right\} + k_{i_5}\int_0^t\left\{f_1^{ref} - p_{c1}k_{d1} - f_1(t)\right\}.d\tau\right)\right].d\tau \end{array}}_{frequencydroopregulation} + \underbrace{\left[k_{p_1}\left[\sum_{n=0}^{N}\left(V_{dc_n}^{*} - V_{dc_n}\right)\right] + k_{i_1}\int_0^t\left[\sum_{n=0}^{N}\left(V_{dc_n}^{*} - V_{dc_n}\right)\right]d\tau\right]}_{dclink}\right] \tag{14}$$

5. Evaluation and Simulation Results

The network system shown in Fig. 1 is implemented on a PSCAD platform, where one microgrid is modelled with wind farm as generation, while others are used as slack bus. The utility grid is connected to the network, which is assumed to be disconnected at certain time, to show the effectiveness of the proposed control.

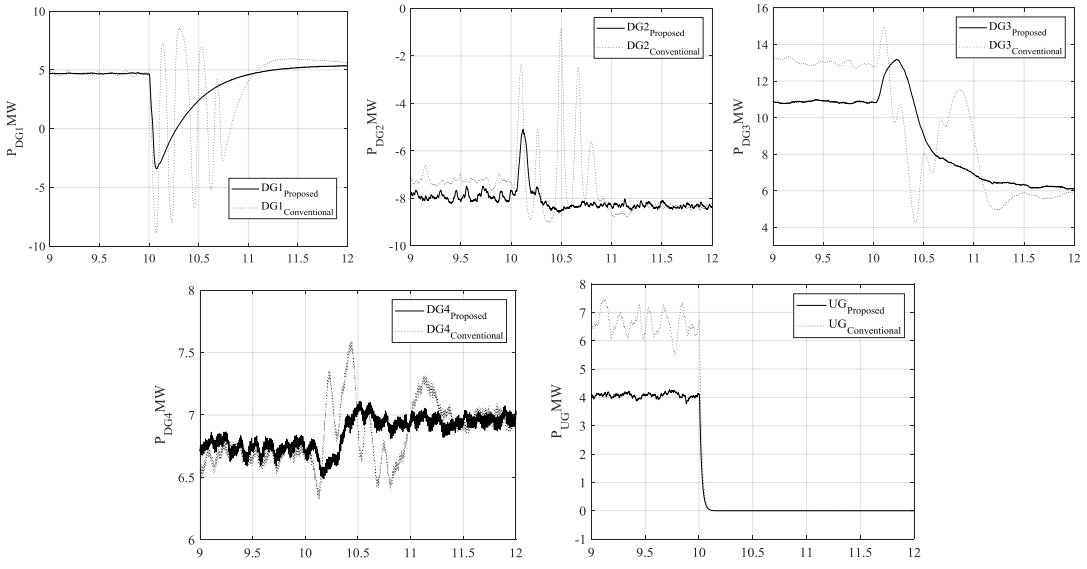

Fig. 3. Power generation of networked microgrids.

5.1. Impact of proposed control on system dynamics

In this case, dynamics of networked system is analysed. The utility grid is simulated to be disconnected at 10s, assuming due to a fault or maintenance reason. The generation of each microgrid, P_{DG1}, P_{DG2},

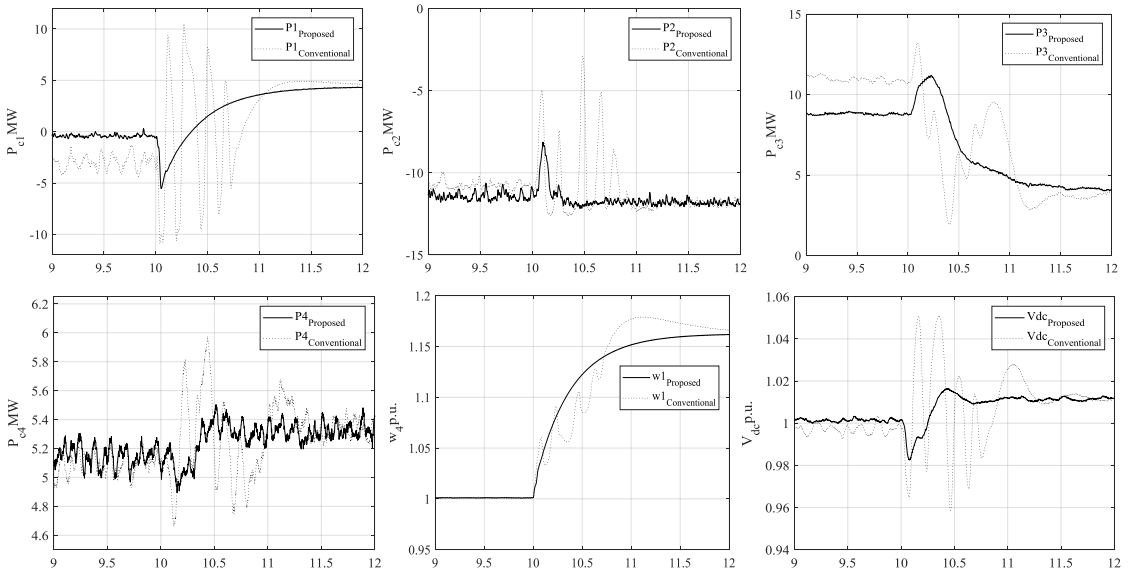

Fig. 4. Power through inverters, generator speed and dc link voltage in networked microgrid.

P_{DG3}, P_{DG4} are shown in Fig. 3, where solid line indicates the proposed control and dotted line indicates conventional method. It is visible that during transition from grid to islanded, the resilience is enhanced with proposed control. Due to the co-ordination of both reference current of inverters, significant improvement is realized.

In Fig. 4, power through inverters, P_1, P_2, P_3, P_4, generator speed, $W_{(pu)}$ and dc link voltage V_{dcpu} is illustrated. It can be seen, the converter power consumption is improved, while speed and dc link voltage fluctuation is reduced.

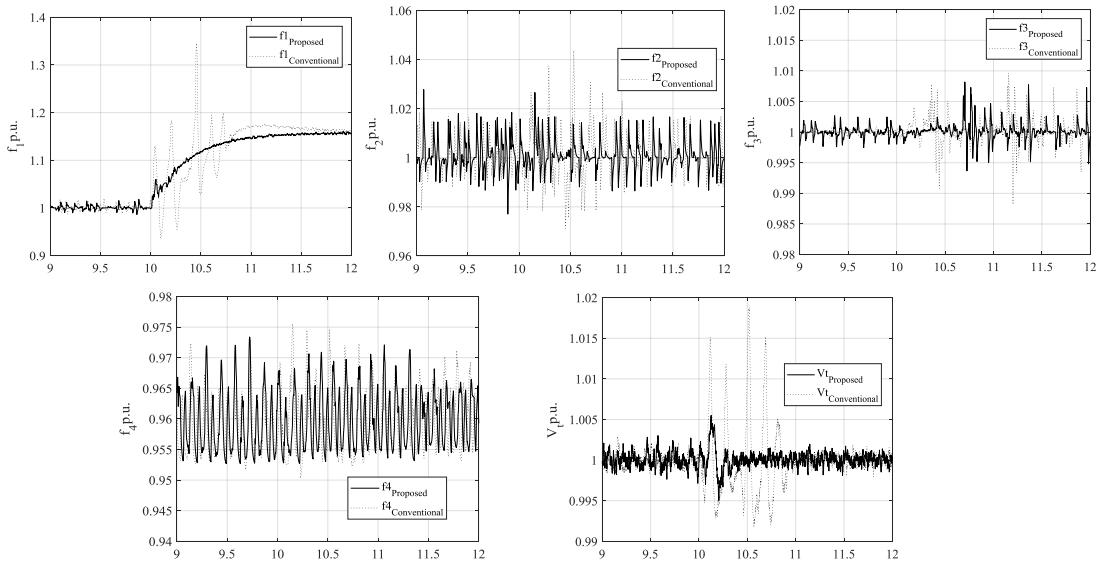

Fig. 5. Responses of system frequency of networked microgrid and terminal voltage.

5.2. Frequency and voltage restoration

The restoration results of system frequency and voltage profile has been shown in this section. Fig. 5 shows that all system level voltages are improved with less fluctuations. The terminal voltage profile is improved as resilience is enhanced with proposed droop control. System frequency of f_1 depicts that it has increased at 10s, due to the droop control system.

6. Conclusion

The paper presents a droop-controlled frequency regulation for a networked microgrid system. The control is applied during transition from grid to islanding mode to enhance the resilience of network. Frequency regulation is applied for microgrid, which provides additional power to the network to balance active power system, through reference current calculation. Moreover, reference current injection is calculated inverters when any microgrid is not able provide additional power. Thus, both reference current injection provides additional resilience to the microgrid in terms of power balance and smooth transition. Simulation results show a comparison between conventional control and proposed control and addresses better performance in the system dynamics and power transfer took place through DC grid. Furthermore, it was shown that partial microgrid increased its generation during islanding to stabilize the system resulting in enhanced power restoration. Thus, a resilient networked microgrid is presented including multiple inverters with coordinated control system.

Conflict of Interest

The authors declare no conflict of interest.

Author Contributions

Mir Nahidul Ambia conducted the research and designed the solutions for his PhD study. The paper was written by Mir, while Ke Meng, Weidong Xiao and Zhao Yang Dong analyzed and reviewed the solutions. Through discussions and different stages of revision, the final paper was approved by all authors.

References

[1] Garba M, Tankari MA and Lefebvre G. Using of distributed energy resources for microgrid resilience achieving. 6th Internal conference on renewable energy research and applications, pp. 659-663, Sad Diego, USA, Nov. 2017.

[2] Liu X, Wang P, and Loh PC. A hybrid AC/DC microgrid and its coordination control. *IEEE Trans. Smart Grid*, Jun.2011; 2(2): 278–286.

[3] Guerrero JM, Chandorkar M, Lee T, and Loh P.C. Advanced control architectures for intelligent microgrids-part I: Decentralized and hierarchical control. *IEEE Trans. Ind. Electron.*, Apr. 2013; 60(4): 1254–1262.

[4] He J, Li WY, Guerrero JM, Blaabjerg F, and Vasquez JC. An islanding microgrid power sharing approach using enhanced virtual impedance control scheme. *IEEE Trans. Power Electron.*, Nov. 2013; 28(11): 5272– 5282.

[5] Guerrero JM, Vasquez JC, Matas J, De Vicuña LG, and Castilla M. Hierarchical control of droop-controlled AC and DC microgrids— A general approach toward standardization. *IEEE Trans. Ind. Electron*., Jan. 2011; 58(1): 158–172.

[6] Nejabatkhah F and Li YW. Overview of power management strategies of hybrid AC/DC microgrid. *IEEE Trans. Power Electron*., Dec. 2015; 30(12): 7072–7089.

[7] Wang Z and Wang J. Self-healing resilient distribution systems based on sectionalization into microgrids. *IEEE Trans. Power Syst*., 2015; 30(6): 3139-3149.

[8] Ambia MN, Hasanien HM, Al-Durra A. and Muyeen SM. Harmony search algorithm-based controller parameters optimization for a distributed-generation system. *IEEE Trans. Power Del.* Feb. 2015; 30(1): 246-255.

[9] Shahnia F, Bourbour S, and Ghosh A. Coupling neighboring microgrids for overload management based on dynamic multicriteria decision-making. *IEEE Trans. Smart Grid*, 2015.

[10] Khorsandi A, Ashourloo M. and Mokhtari H. A decentralized control method for a low-voltage DC microgrid. *IEEE Trans. Energy Convers*., Dec. 2014: 29(4); 793–801.

[11] Ambia MN, Al-Durra A. and Muyeen SM. Centralized power control strategy for ac-dc hybrid microgrid system using multi-converter scheme. *IECON 37th Annual conference of the IEEE Industrial Electronics*, pp. 843-848, Melbourne, Australia, 2011.

[12] Farrokhabadi M, Caizares CA, and Bhattacharya K. Frequency control in isolated/islanded microgrids through voltage regulation. *IEEE Trans. on Smart Grid,* May 2017; 8(3): 1185-1194.
[13] Wang Z, Chen B, Wang J, and Chen C. Networked microgrids for self-healing power systems. *IEEE Trans. Smart Grid*, Jan. 2016; 7(1): 310-319.